JOURNAL OF MATERIALS SCIENCE : MATERIALS IN MEDICINE 3 (1992) 229–233

Transformation characteristics and related deformation behaviour in orthodontic NiTi wire

M. THIER, D. TREPPMANN
Institut für Werkstoffe, Ruhr-Universität Bochum, D-4630 Bochum, Germany
D. DRESCHER, C. BOUREAUL
Poliklinik für Kieferorthopädie, Rheinische Friedrich-Wilhelms-Universität, Bonn, Germany

Several orthodontic NiTi wires have been investigated by differential scanning calorimetry measurements and uniaxial tensile tests. An attempt is made to relate pseudoelastic deformation behaviour to characteristics of diffusionless martensitic transformation. Pseudoelasticity is explained by the respective importance of each parameter for use in orthodontics and experimental results are presented in terms of classification.

1. Introduction

Since their introduction to orthodontics by Andreasen in 1971 [1], NiTi wires have been extensively used. The unique elastic properties of these alloys have been further enhanced, especially with respect to their pseudoelastic properties [2–4].

NiTi, as an intermetallic compound in near equilibrium condition, seems to fulfil the biological requirements in function and biocompatibility. The combination of a large working range, constant force, small modulus of elasticity, and a high degree of biocompatibility make them especially suited for orthodontic as well as medical purposes [5–10].

Concerning the various orthodontic NiTi alloys currently in use, there is little information about their transformation characteristics and related deformation properties. Thermal analysis techniques have been previously used to reveal transformation characteristics in these alloys [11, 12]. To characterize the NiTi orthodontic wires currently in use, which display remarkably different pseudoelastic properties, the transformation temperatures as well as deformation parameters have now been investigated.

2. Experimental procedure

Several orthodontic wires were obtained from commercial sources, as explained in Table I.

Transformation temperatures were measured using a Du Pont 2100 differential scanning calorimeter (DSC). Samples of mass 0.05–0.1 g, which were cut from the orthodontic wires, were placed in an aluminium crucible. The heating/cooling rate was 10 °C min^{-1}. Since the A_s-temperature, i.e. the temperature of the commencement of reverse transformation, was detectable in nearly all the samples, it was taken as the characteristic temperature for each wire. As it is difficult to accurately detect the beginning of transformation from the point of departure from the base line, the extrapolation onset point is assumed to be the temperature of transformation commencement.

Uniaxial tensile tests were performed by using a Zwick 1387 universal testing machine. The gauge length of the specimen was 40 mm. All tests were carried out at a strain rate of $10^{-4}\ s^{-1}$, while the test temperature was held at 37 °C. The samples were deformed up to the very end of the pseudoelastic plateau, and then unloaded at a strain rate of again $10^{-4}\ s^{-1}$.

3. Results

DSC curves obtained from various orthodontic wires can be classified into three categories, depending on whether the martensitic transformation and the reverse transformation (Fig. 1), the reverse transformation (Fig. 2), or finally no transformation (Fig. 3) is detectable in DSC scanning. A complete classification and the A_s-temperature of each sample, if detectable, are given in Table II.

TABLE I Orthodontic NiTi wires

Abbreviation	Product	Company
AOT	Memorywire NiTi	American Orthodontics
DNT	Rematitan Lite	Dentaurum
FTS	Titanol Superelastic	Forestadent
NIS	Nitinol SE	Unitek
NIT	Nitinol	Unitek
ONI	NiTi	Ormco
OSN	SuperNitane	Ormco
RMO	Orthonol	Rocky Mountain
RMT	Rematitan	Dentaurum
SSA	Sentalloy	Soar
TXR	Titanal XR	Lancer

0022–2461

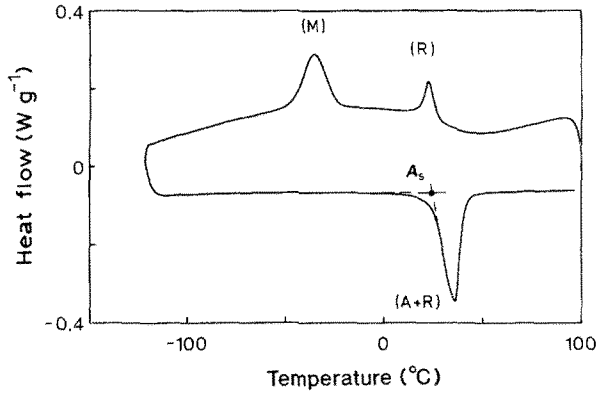

Figure 1 DSC curve of SSA sample, showing transformation signals from martensitic (M) and reverse (A) transformation; R-phase transformation is marked by (R).

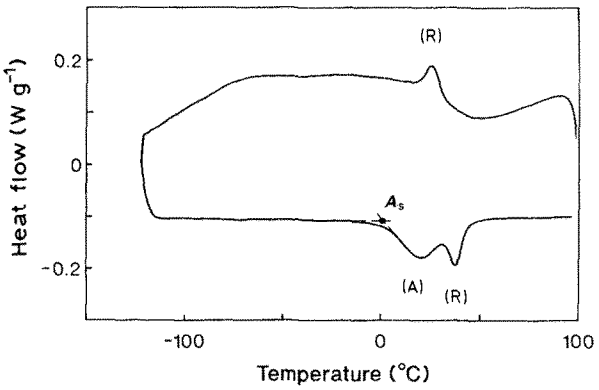

Figure 2 DSC curve of ONI sample, where reverse transformation (A) to the austenite is visible; R-phase transformation is marked by (R).

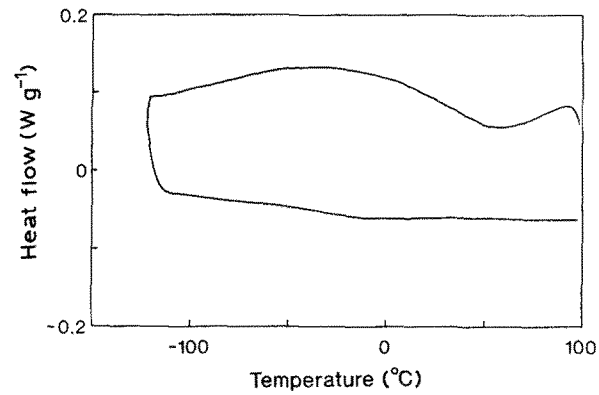

Figure 3 DSC curve of RMO sample. No transformation signal is detectable.

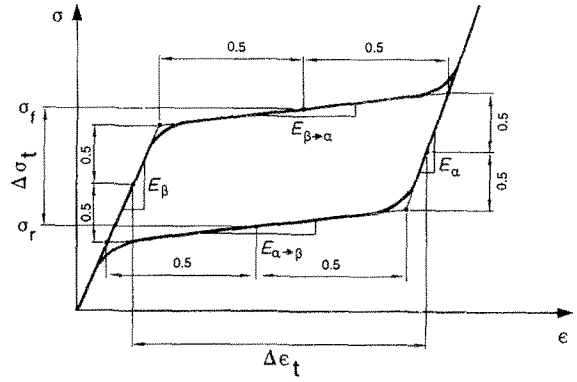

Figure 4 Pseudoelastic deformation curve and definitions, which were used in examination of stress-induced transformation characteristics. Parameters in this investigation: flow stress (σ_f) of martensitic transformation, flow stress (σ_r) of reverse transformation, hysteresis ($\Delta\sigma_t$) in stress, hysteresis ($\Delta\varepsilon_t$) in strain, slope ($E_{\beta\to\alpha}$) in transformation stress, slope ($E_{\alpha\to\beta}$) in reverse transformation stress.

TABLE II Classification and A_s-temperatures of orthodontic NiTi wires after DSC scanning

Classification	Sample	A_s(°C)
Type I	DNT	− 20
(martensitic transformation	SSA	+ 15
and reverse transformation)		
Type II	AOT	− 20
(reverse transformation)	FTS	− 15
	NIS	(− 20)
	NIT	(0)
	ONI	− 10
	OSN	− 25
	TXR	(− 15)
Type III	RMO	–
(no transformation)	RMT	–

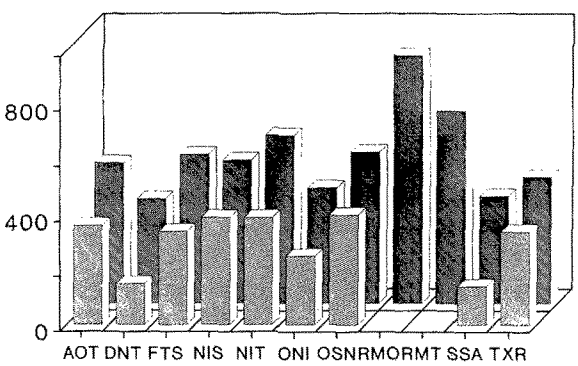

Figure 5 Experimental results in formation flow stress (σ_f) and reverse transformation stress (σ_r) in orthodontic NiTi samples. (▨) Reverse stress (MPa), (■) flow stress (MPa).

Examination of stress–strain curves has been carried out according to the definitions presented in Fig. 4. Results obtained in flow stress measurements, associated with formation and reverse transformation of martensite, are summarized in Fig. 5. Characteristic hysteresis in stress and strain of almost all samples are presented in Fig. 6. However, instead of a near constant stress level in the pseudoelastic plateau during reversible martensitic transformation, significant alterations in stress level have been ascertained (Fig. 7).

4. Discussion

4.1. Transformation characteristics

Differences obtained in DSC curves may be explained by the influence of cold working on the transformation behaviour.

It has been revealed by electrical resistance measurements that an increasing amount of deformation will diminish the transformation signal. If a critical amount of deformation is exceeded, no signal from

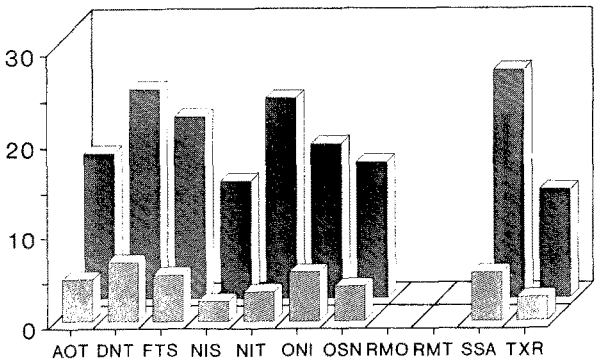

Figure 6 Stress ($\Delta\sigma_t$) and strain ($\Delta\varepsilon_t$) hysteresis in orthodontic NiTi samples. (▨) Strain (%), (■) stress (10^{-1} MPa).

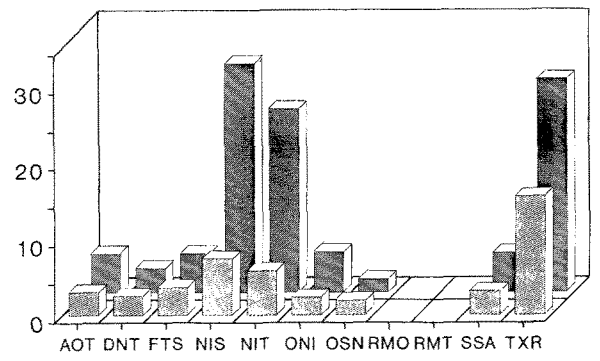

Figure 7 Slope in stress during formation ($E_{\beta\to\alpha}$) and reverse transformation ($E_{\alpha\to\beta}$) of martensite in orthodontic NiTi samples. (▨) Martensite formation (MPa/%), (■) reverse transformation (MPa/%).

transformation behaviour can be detected [13]. By using DSC measurements, it has been shown that additional heat treatment after cold working will reveal the characteristics of NiTi transformation behaviour [14].

Thus, orthodontic NiTi wires, classified in Table II (types I–III), may have been treated by an increasing amount of deformation or at a decreasing temperature (types I–III) during heat treatment after cold working. This suggests that the amount of irreversible deformation retained in the material is measurable by the magnitude of transformation signals, whether they were taken from electrical resistance measurements or DSC scanning.

4.2. Pseudoelastic behaviour in orthodontics

The deformation behaviour of pseudoelastic NiTi wires offers distinct advantages for the correction of tooth position in orthodontic applications. It is possible to carry out corrective movement by a driving force at a physiological level, by using the large working range of these materials, and to realize a complete correction treatment on an almost constant stress level. A method to describe pseudoelastic material has been introduced, and is shown in Fig. 4.

In orthodontic application, the feature of importance in the pseudoelastic hysteresis is the reverse transformation from stress-induced martensite (α) to austenite (β). Whereas an orthodontic wire is activated during martensite formation ($\beta \to \alpha$), the driving force for corrective movement (see Fig. 5) is taken from the reverse transformation to the austenite ($\alpha \to \beta$). Since the application in orthodontics is that of bending, the change in stress state has to be taken into consideration [15].

The stress hysteresis only describes the difference between activation stress and stress level used for corrective movement, whereas, the strain hysteresis determines the limits of the working range of each NiTi wire (Fig. 6). A great hysteresis in strain will ensure that the correction treatment will be carried out at one physiological stress level.

Among these factors important to the use of pseudoelasticity in orthodontics, there is at least one that describes the decrease in driving force during corrective movement (Fig. 7). As has been indicated above, the alteration of stress during formation and reverse transformation of martensite also seems to be related to the prior treatment of the alloy. The effect of alloy treatment and the consequences for the characteristics of pseudoelasticity will now be discussed.

4.3. Alloy treatment

Three types of DSC scans have been classified depending on whether martensitic and reverse transformation, martensitic transformation, or no transformation signal were detectable (Table II).

The observation of martensitic as well as reverse transformation in type I DSC scans indicates that there will be only a small amount of irreversible plastic deformation in this material. Characteristics of deformation behaviour in type I material (DNT, SSA) are the lowest flow stress in the formation and in the reverse transformation of martensite and the largest hysteresis in stress which has been measured (Figs 5, 6).

Type II DSC scans may be characterized by an intermediate amount of residual plastic deformation, after final heat treatment. No such significant features can be drawn out here as for type I scans. There is a similar behaviour in pseudoelasticity in type II material, except three samples, which can be identified by the poor signal in DSC scanning. Characteristics in pseudoelastic behaviour of this part of type II material (NIS, NIT, TXR) were registered in the alteration of stress, during formation and reverse transformation of martensite. Among the other pseudoelastic materials (type II), these samples, characterized by the poorest but detectable signal in differential scanning calorimetry, show a significant alteration of stress in the pseudoelastic plateau (Fig. 7).

The absence of all transformation signals, caused by a large amount of irreversible plastic deformation, characterizes type III material (Fig. 3). As a consequence of that, no pseudoelastic characteristic could be found in such material (RMO, RMT). Thus a significantly high flow stress is detected (Fig. 5) and subsequent deformation obviously is of an irreversible, plastic manner. As a result of material treatment,

there will be no hysteresis and no pseudoelastic plateau to measure (Figs 6, 7).

4.4. Tendencies

With the exception of type III material, the temperature at the beginning of reverse transformation (A_s) was detectable in all samples. Characteristic tendencies can be taken from results obtained in tensile experiments, if pseudoelastic features were related to A_s transformation temperatures.

As a result of increasing A_s-temperature, there will be a decrease in flow stress; a lower critical driving force is then needed for stress-induced formation of martensite (Fig. 8). Furthermore, stress hysteresis as well as strain hysteresis will be enlarged by an increase in A_s-temperature (Figs 9, 10). Therefore, depending on A_s-temperatures, deformation experiments will lead to characteristic changes in stress–strain behaviour. A generalizing illustration of this observation is given in Fig. 11.

Although these tendencies of pseudoelastic behaviour in relation to transformation characteristics could have been shown, there is a complex amount of specific phenomena underlying this. It has to be pointed out that the flow stress as well as the hysteresis in stress and strain are considerably influenced by material composition and material treatment.

For instance, it has been already evaluated that each parameter will reveal its own characteristic influence on relating transformation behaviour [16]. Further investigations on the effect of cold working, heat treatment, and alloy composition are intended. Nevertheless, specified transformation characteristics and associated mechanical properties will define pseudoelastic behaviour of NiTi alloys.

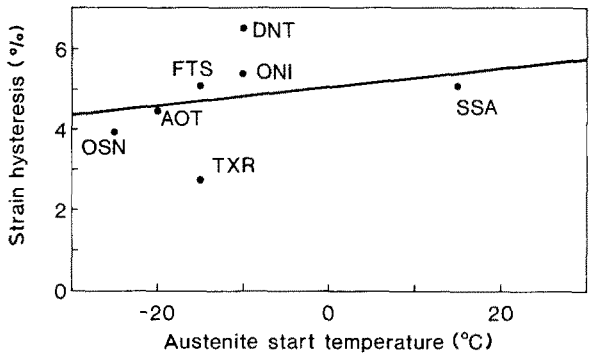

Figure 10 Tendency obtained, when strain hysteresis ($\Delta\varepsilon_t$) is related to beginning reverse transformation temperature (A_s).

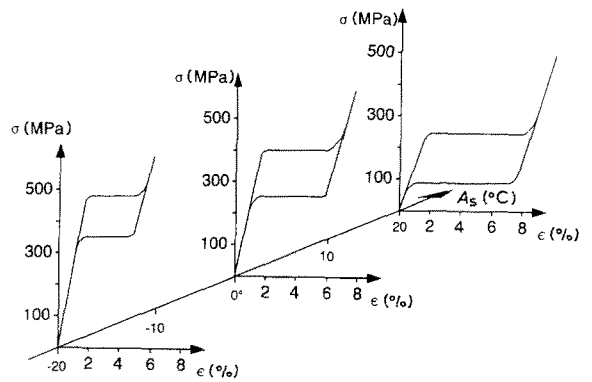

Figure 11 Generalizing illustration of tendencies obtained, if flow stress (σ_f) and hysteresis in stress ($\Delta\sigma_t$) and strain ($\Delta\varepsilon_t$) are related to the beginning reverse transformation into austenite. ($T = 37\,°C$).

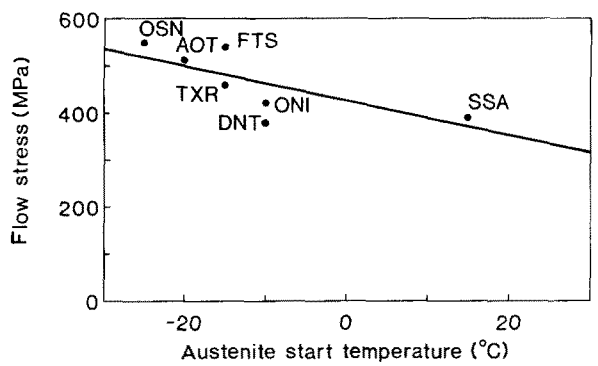

Figure 8 Tendency obtained, when flow stress (σ_f) is related to beginning reverse transformation temperature (A_s).

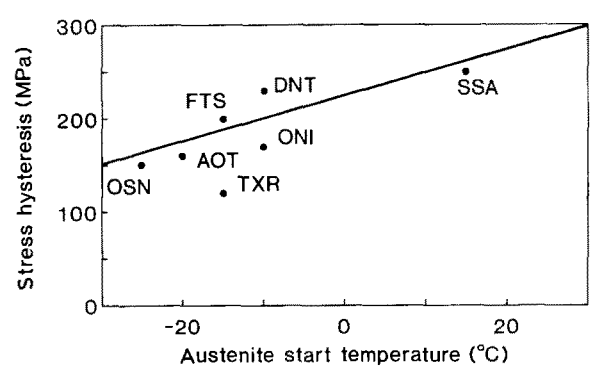

Figure 9 Tendency obtained, when stress hysteresis ($\Delta\sigma_t$) is related to beginning reverse transformation temperature (A_s).

5. Conclusions

A classification in DSC scanning is made according to whether there is a signal from martensitic and reverse transformation, from reverse transformation, or where no transformation signal is to be detected. The reverse transformation temperature (A_s) is suggested to be the characteristic temperature of transformation behaviour.

It is possible to reveal tendencies in flow stress as well as in hysteresis of stress and strain, when these pseudoelastic features are related to the A_s-temperature. However, according to the transformation characteristics and resulting pseudoelastic behaviour, there is the need for further investigations to separate the influence of alloy composition, cold work, and heat treatment.

Acknowledgements

The authors acknowledge the German Research Foundation for project support.

References

1. G. F. ANDREASEN and T. B. HILLEMAN, *J. Amer. Dent. Assoc.* **82** (1971) 1373.
2. G. F. ANDREASEN, H. HEIMAN and D. KRELL, *Angle Orthod.* **55** (1985) 120.
3. C. J. BURSTONE, B. QIN and J. Y. MORTON, *Amer. J. Orthod.* **87** (1985) 445.
4. F. MIURA, M. MOGI, Y. OHURA and H. HAMANAKA, *Amer. J. Orthod. Dentofac. Orthop.* **90** (1986) 1.
5. F. MIURA, M. MOGI, Y. OHURA and M. KARIBE, *ibid.* **94** (1988) 89.
6. F. BAUMGART, G. BENSMANN, J. HAASTERS, A. NÖLKER and K. F. SCHLEGEL, *Arch. Orth. Traum. Surg.* **91** (1978) 67.
7. G. BENSMANN, F. BAUMGART and J. HARTWIG, *Metall.* **35** (1981) 312.
8. G. von SALIS-SOGLIO, *Z. Orthop.* **127** (1989) 191.
9. L. S. CASTLEMAN and S. M. MOTZKIN, in "Biocompatibility of clinical implant materials", edited by D. F. Williams (CRC Press, Boca Raton, FL, 1981) p. 129.
10. X. ZHANG, G. LIU, J. YUEN, Q. ZAO, L. YI, Z. HU, S. ZHOU and J. HUO, in Proceedings of the International Symposium on Shape Memory Alloys, Guilin, September 1986, edited by Y. Chu, T. Y. Hsu and T. Ko (China Academic Publishers, Guilin, 1986) p. 416.
11. D. P. DAUTOVICH, Z. MELKVI, G. R. PURDY and C. V. STAGER, *J. Appl. Phys.* **37** (1966) 2513.
12. J. H. LEE, J. B. PARK, G. F. ANDREASEN and R. S. LAKES, *J. Biomed. Mater. Res.* **22** (1988) 573.
13. Y. ZHANG and E. HORNBOGEN, *Z. Metallkde* **78** (1987) 401.
14. T. TODOROKI and H. TAMURA, *Trans. Jpn. Inst. Metals* **28** (1987) 83.
15. M. THIER, *J. Mater. Sci.*, in press.
16. E. HORNBOGEN, *Acta Metall.* **33** (1985) 595.

Received 28 January
and accepted 21 May 1991